

Spin current through an ESR quantum dot: A real-time studyLei Wang,¹ Hua Jiang,¹ J. N. Zhuang,¹ Xi Dai,¹ and X. C. Xie^{2,1}¹*Beijing National Laboratory for Condensed Matter Physics and Institute of Physics, Chinese Academy of Sciences, Beijing 100190, China*²*Department of Physics, Oklahoma State University, Stillwater, Oklahoma 74078, USA*

(Received 24 September 2009; revised manuscript received 4 February 2010; published 26 February 2010)

The spin transport in a strongly interacting spin-pump nanodevice is studied using the time-dependent variational-matrix-product-state approach. The precession magnetic field generates a dissipationless spin current through the quantum dot. We compute the real-time spin current away from the equilibrium condition. Both transient and stationary states are reached in the simulation. The essentially exact results are compared with those from the Hartree-Fock approximation (HFA). It is found that correlation effect on the physical quantities at quasisteady state are captured well by the HFA for small interaction strength. However the HFA misses many features in the real-time dynamics. Results reported here may shed light on the understanding of the ultrafast processes as well as the interplay of the nonequilibrium and strongly correlated effect in the transport properties.

DOI: [10.1103/PhysRevB.81.075323](https://doi.org/10.1103/PhysRevB.81.075323)

PACS number(s): 75.25.-j, 03.67.Lx, 73.23.-b, 85.35.Be

I. INTRODUCTION

The rapid progress of nanoelectronics and information technologies has prompted intense interest in exploiting the spin properties of the electrons, which results in the emergence of spintronics.¹ One of the most important spin-based electronic devices is a mesoscopic quantum dot (QD) system. Spin-polarized transport through a QD has been extensively investigated recently. It has been shown theoretically² and demonstrated experimentally³ that a QD system will function as a phase-coherent spin pump in the presence of sizable Zeeman splitting. Very recently, spin-polarized current has been detected from a quantum point contact⁴ and from Coulomb-blocked QDs.⁵ The electron spin resonance QD (ESR-QD) could also serve as an element device for quantum computing.⁶

Due to its small size, Coulomb correlation could play important role in the transport experiments involving a QD. At low temperature, Kondo effect creates new states with many-body character at the Fermi level. Although the effect of Kondo resonance on the charge current has been studied in the QD for different situations, its influence on the spin current is less known. The physical processes involved in the transport experiments are out of equilibrium in many cases. Moreover, the state of the system may also be time dependent. These features make the investigations inaccessible from the conventional many-body tools. So an essentially exact numerical method for the nonequilibrium and time-dependent phenomena in the interacting nanodevices is highly desirable, which can also verify the approximations used in various analytical approaches.

There exist several powerful methods to deal with the low-dimensional-correlated systems, such as the numerical renormalization group (NRG) and the density-matrix renormalization group (DMRG). With the input from the quantum-information science, time-evolving block decimation (TEBD) (Refs. 7 and 8) and adaptive time-dependent DMRG (t-DMRG) have received much attention.^{9,10} To our knowledge, there are some previous studies of the nonequi-

librium transport of the nanodevices using the adaptive t-DMRG technique.¹¹⁻¹³ By adopting the logarithmic discretization,¹⁴ have studied the Kondo correlations.¹⁵ have examined the noninteracting resonant level model in the Landau-Zener potentials. Besides the adaptive t-DMRG approach, there are also attempts based on the time-dependent NRG,¹⁶ functional RG,¹⁷ Dyson equation embedding,¹⁸ flow-equations,^{19,20} and quantum Monte Carlo²¹⁻²³ methods. But the adaptive t-DMRG approach gives direct access to the transient regime and could handle the time-dependent Hamiltonian directly. The time-dependent variational product state (tVMPS) approach adopted in this paper is directly connected with the adaptive t-DMRG (Refs. 9 and 10) and the TEBD (Refs. 7 and 8) approaches. The computational cost of these two methods is very similar, and in practice both methods achieve a similar accuracy.²⁴

The merit of the VMPS approach lies in two aspects. First, it represents a large class of states, which could be seen from the success of the NRG and DMRG approaches [which generate matrix product states (MPS) in their processes] for the zero and one-dimensional quantum models. And the fact that the entanglement entropy increases slowly in one dimension also permits one to simulate the states classically using the VMPS method.²⁴ Second, it is easier to handle the MPS, i.e., the overlap of two MPS, the expected value of an operator in a given MPS, etc., can be calculated with polynomial complexity.

In this paper we study the spin current through an ESR quantum dot with Coulomb interaction.²⁵⁻²⁷ We obtain the transient as well as the quasisteady state spin current using the time-dependent VMPS method. We also studied the effect of the interacting on the spin current. The results are compared with time-dependent Hartree-Fock approximation (TD-HFA) and nonequilibrium Green's function (NEGF) approach for the quasisteady state.

II. MODEL

We consider an ESR setup of a quantum dot, where single-electron level of the dot is split by the Zeeman field B_0

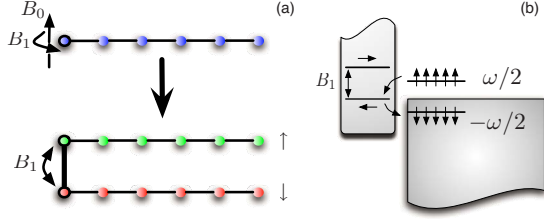


FIG. 1. (Color online) (a) The experimental setup of an ESR quantum dot. Besides the Zeeman field B_0 along the z axis, there is a rotational magnetic field B_1 acting in the xy plane. The dot is coupled to a noninteracting lead and forms a SIAM chain. The SIAM chain is unfolded into two spinless chains, and they are coupled at the leftmost end by Coulomb interaction U and the rotational magnetic field B_1 . (b) Schematic view of time-independent energy levels in the rotational reference frame. The Fermi level of the spin up/down electrons in the lead is shifted to $\pm\omega/2$, while the $|\leftarrow\rangle$ and $|\rightarrow\rangle$ levels in the dot split by $2g\mu_B B_1$. The dot levels could be tuned by the gate voltage V_g .

and the two spin levels are coupled by a rotating magnetic field $B_1[\cos(\omega\tau), \sin(\omega\tau)]$. The Hamiltonian reads $H = H_{\text{dot}} + H_{\text{rotate}} + H_{\text{lead}}$

$$H_{\text{dot}} = V_g \sum_{\sigma} n_{\sigma} - \frac{g\mu_B B_0}{2} (n_{\uparrow} - n_{\downarrow}) + U n_{\uparrow} n_{\downarrow},$$

$$H_{\text{rotate}} = -\frac{g\mu_B B_1}{2} (d_{\uparrow}^{\dagger} d_{\downarrow} e^{i\omega\tau} + d_{\downarrow}^{\dagger} d_{\uparrow} e^{-i\omega\tau}),$$

$$H_{\text{lead}} = -t' \sum_{\sigma} (d_{\sigma}^{\dagger} c_{1,\sigma} + \text{H.c.}) - t \sum_{i=1;\sigma}^{N_{\text{lead}}} (c_{i,\sigma}^{\dagger} c_{i+1,\sigma} + \text{H.c.}). \quad (1)$$

Here d and c denote the annihilation operator of electron in the dot and the lead. H_{lead} contains the terms describing coupling of the dot with the lead and the hopping in the lead. H_{rotate} contains the rotating magnetic field. H_{dot} contains the Zeeman splitting, the gate voltage terms and the on-site Coulomb repulsion between the spin-up and -down electrons. In the present study we fix $t=1$ and $g\mu_B B_0 = \omega = 1$ where the ESR resonance condition is satisfied. We set $g\mu_B B_1 = 2$ and $t' = 0.4$ unless mentioned. The single lead is a noninteracting chain with N_{lead} sites. The coupling of it with the QD is described by the hybridization $\Gamma = \pi t'^2 \rho$.

III. METHODS

The time dependence of the Hamiltonian could be eliminated by the unitary transformation $U = e^{-i(\omega\tau/2)[\sum_i (c_{i,\downarrow}^{\dagger} c_{i+1,\downarrow} + c_{i+1,\downarrow}^{\dagger} c_{i,\downarrow}) + (d_{\uparrow}^{\dagger} d_{\downarrow} - d_{\downarrow}^{\dagger} d_{\uparrow})]}$. It transforms the Hamiltonian into rotating reference frame (RF), see Fig. 1(b). One can see that the rotating magnetic field, in effect, shifts lead electron energy to the opposite directions for up and down spins. Quasisteady state spin current has been studied in the RF using the NEGF method in the noninteracting and infinite U case²⁵ and by NRG approach²⁷ in adiabatic limit. In the following we will revisit the problem in transient as well as

quasisteady regime, and treat the interacting nonperturbatively with the exact numerical methods.

For the time-dependent Hamiltonian $H(\tau)$, the evolution of the density matrix ρ follows the von Neumann equation $i\frac{d\rho}{d\tau} = [H, \rho]$. For the noninteracting case, one could write $H(\tau)$ with the single-particle basis. Then direct integration of the von Neumann equation with a given initial condition $\rho(\tau)|_{\tau=0} = \rho_0$ could be easily done. The initial density matrix ρ_0 is calculated from ground state of the single impurity Anderson model (SIAM) chain without the rotating magnetic field B_1 .

From the density operator $\rho(\tau)$ the occupation on the dot is calculated by $n_{\sigma}(\tau) = \langle \psi(\tau) | d_{\sigma}^{\dagger} d_{\sigma} | \psi(\tau) \rangle$, and the spin current through the dot is $J^{\sigma} = \frac{2e}{\hbar} \text{Im}[t' \langle \psi(\tau) | d_{\sigma}^{\dagger} c_{1,\sigma} | \psi(\tau) \rangle]$, i.e., they are evaluated on the bond connect the dot and the lead. We set $g\mu_B = e = \hbar = 1$ in this paper.

For the interacting case we adopt the VMPS approach to calculate the ground state of $H(\tau=0)$. Then we apply the rotational magnetic field B_1 on the dot at $\tau=0$, and perform the time evolution.²⁸ To reduce the dimension of the local Hilbert space, an unfolded technique²⁹ is used, the original SIAM chain is unfolded into two chains with different spins. The total length of the unfolded SIAM chain is L . They are connected at the end point by the Coulomb repulsion and the rotating magnetic field B_1 . The errors of the computation mainly come from the following sources. First the Trotter decomposition error. Second the truncation errors accumulated in the course of the time evolution. For short-time scale the Trotter error dominates while for the long time the truncation error dominates. Caution must also be taken because of the finite size of the leads. The electrons may bounce at the end point and the spin current flows along the reverse direction. This is an artifact of the present method and could be eliminated by careful finite-size scaling analysis.

We also use TD-HFA method to investigate the interacting case approximately, in which the interaction term is factorized into $U(\langle n_{\uparrow} \rangle n_{\downarrow} + n_{\uparrow} \langle n_{\downarrow} \rangle)$. At each time step of the integration of the von Neumann equation, the dot occupation which is used to update the Hartree-Fock Hamiltonian. This approach is as efficient as the noninteracting cases.

IV. RESULTS

In Fig. 2 we show the development of the spin current after the rotational magnetic field B_1 is applied to the noninteracting dot. To reduce the transient region, we use a larger coupling constant $t'=1$ here. For small chain length ($L=8, 16$) the finite-size effect shows up within the maximum time of our simulation. The charge pulse reaches the end of the chain and bounces back thus causes the reversing of the sign of the spin current. However, the spin current reaches a saturation value for larger chain length ($L=8, 16$), which indicates the quasisteady state spin transport is achieved. In the quasisteady state, the spin-up electrons flow in the dot, flip their spins and then flow away. There is no net charge transport since $J_{\uparrow} = -J_{\downarrow}$. Overshooting behavior at short-time scales ($\tau \sim 1.8$) is observed. It is due to abrupt applying of the rotational magnetic field and could be suppressed if the rotational magnetic field is turned on adiabatically. The

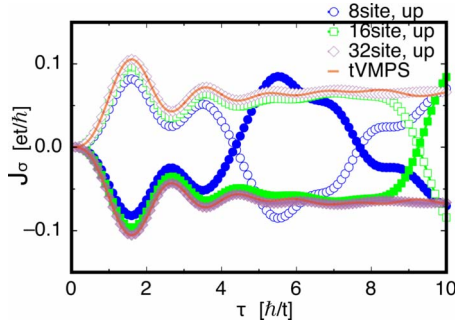


FIG. 2. (Color online) The spin current for different chain length $L=8, 16, 32$. The (red) solid line is the tVMPS result and the dots are from direct integration of the von Neumann equation, see text. Quasisteady state could be recognized for larger chain length. Where J_{\uparrow} (hollow dots) and J_{\downarrow} (filled dots) are of opposite sign.

tVMPS result for $L=32$ nicely follows the direct integration of the von Neumann equation. The oscillation at long times in the tVMPS approach was also noticed in the previous study with the adaptive t-DMRG approach.¹¹ With the increasing of the bond dimension, the oscillation tends to disappear. The coincidence validates the VMPS method for the noninteracting case. However, its main power lies in the interacting cases and we expect similar precision could be achieved in that case.

Electron occupation and spin current through the quantum dot are calculated as functions of time for different gate voltages V_g , shown in Fig. 3. It is seen that the overall occupation on the dot oscillates as it reaches its quasisteady-state value, the spin current develops in the mean time. Note that the transient state current can even be of the opposite sign with its value in the quasisteady state, Fig. 3(b). By taking

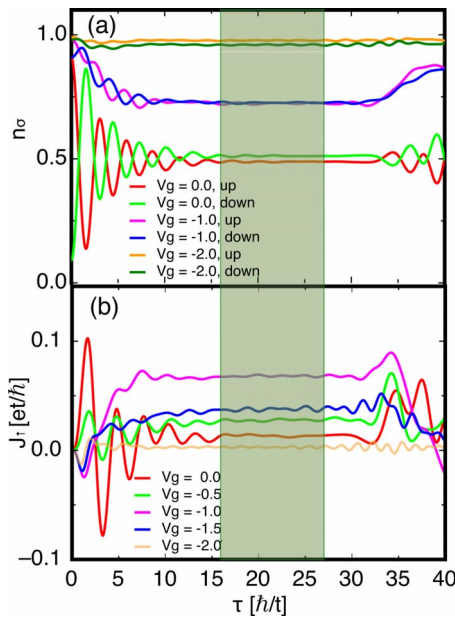


FIG. 3. (Color online) Dot occupancy for each spin (upper panel) and spin current (lower panel) for a 64 sites chain with different gate voltage. The shaded region is averaged to calculate the quasisteady state spin current.

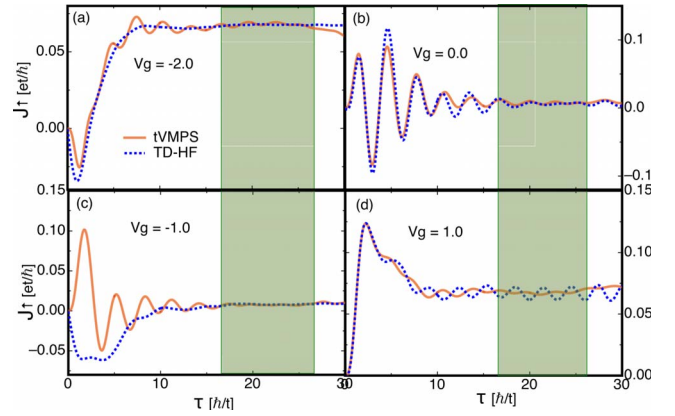


FIG. 4. (Color online) The comparison of the tVMPS (full line) and TD-HFA (dot line) results of spin current for different gate voltage, where the interacting strength $U=1$. The shaded area is averaged to give the quasisteady state current.

average of physical quantities in the quasisteady state, we extract variation in the quasisteady-state dot occupation and spin current with the gate voltage V_g , see Fig. 5. The spin polarization in the steady state is less pronounced than the initial state. And it is even inverted for $-1 < V_g < 1$, Fig. 5(a). The steady-state current attains its maximum value at $V_g = \pm 1$. This is the case where $n_{\uparrow} = n_{\downarrow}$, i.e., the dot is spin unpolarized. It can be seen from Fig. 1(b), in this case $V_g \pm B_1 = 0$ and the $|\leftarrow\rangle$ ($|\rightarrow\rangle$) is tuned to zero-energy point. Spin-flip process on the dot is most efficient and gives a maximum spin current. We also use NEGF to study the current and occupation in the RF, see inset of Fig. 5(a). It gives qualitatively similar results, the small discrepancy is due to the finite-size effect of the tVMPS approach. It should be noted that NEGF approach adopted here does not yield results of transient state since the unitary transformation eliminates the time dependence. To take into account the initial condition properly, the two-time Green's function should be used.^{30–32}

For interacting case, we calculate the real-time spin current through the ESR-QD by tVMPS method. The results were compared with TD-HFA results, see Fig. 4 for $U=1$. Although there are discrepancies in the real-time data, the TD-HFA captures the overall behavior of the spin current. This is due to the Kondo physics—which is missing from the TD-HFA approach—does not manifests itself here since the presence of large magnetic field B_1 and Fermi-surface splitting in the lead. Kondo effect may be restored when B_1 is reduced below Kondo temperature.²⁷ But small B_1 also reduce the chance of spin-flip process on the QD, thus reduce the spin current through it. Surprisingly, the average of physical quantities in the quasisteady state of these two approaches are in good agreement, see Fig. 5. Based on this investigation, we validate that the HFA is a good approximation for the qualitative investigation of spin-pump devices away from the Kondo regime. However, caution must be taken when it is used to make prediction on the real-time dynamics. For example, for the $V_g = -1.0$ case, the transient state spin current of TD-HFA is of the opposite sign to the tVMPS prediction, thus it is quantitative wrong.

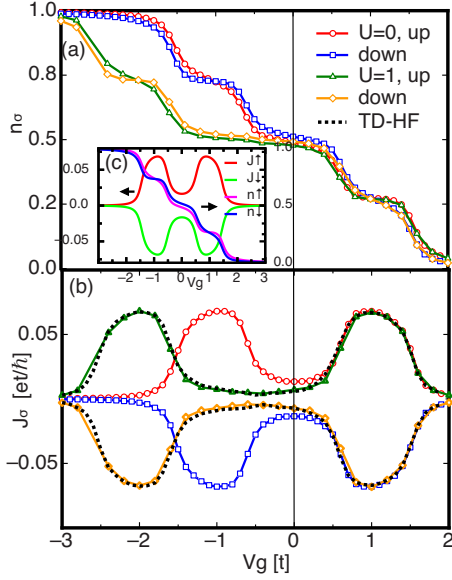


FIG. 5. (Color online) Occupation of electrons on the dot (upper panel) and spin current through the dot (lower panel) for different gate voltages. The spin current of high filling region is not affected by the interacting, while the spin current peak at low filling is shifted by U . Inset are the $U=0$ quantities calculated in rotational reference frame by NEGF approach.

The magnitude of spin current with the gate voltage is still a two-peaked curve similar to the noninteracting case. Interaction has different effects on the high and low filling regimes of the dot, Fig. 5(b). It does not modify the dot occupation and the spin current dramatically for $V_g > 0$. The peak of the spin current remains at $V_g = 1$ and the maximum value is only suppressed by one percent up to $U = 3$. However, since the average dot occupation is larger than 1 for $V_g < 0$, the correlation effect shifts the spin current peak downwards by U . This is a manifestation of the Coulomb blockade effect.

The fluctuation of the density $\Delta = \langle \delta n_\uparrow \delta n_\downarrow \rangle = \langle n_\uparrow n_\downarrow \rangle - \langle n_\uparrow \rangle \langle n_\downarrow \rangle$ is also calculated. It is a measure of the accuracy of the HFA approach. This quantity is conserved under the particle-hole transformation. Thus two different gate voltages

satisfying $V_g + V'_g = -U$ give the same value of Δ . This is respected in the tVMPS calculation. But the discrepancy from the tVMPS is unrelated to it, i.e., although $V_g = 1$ and 0 has the same Δ , the discrepancy of the spin current from the tVMPS result is not the same. We find the HFA is surprisingly good for the quasisteady state physical quantities even if the fluctuation is relatively large. The fluctuation is always negative due to the Cauchy-Schwarz inequality, indicating that the HFA overestimates the potential energy. The absolute value of the fluctuation reaches its maximum 0.2 for $-1 < V_g < 0$. However, even for these cases, the HFA data still shows good agreement with the tVMPS data.

V. CONCLUSION

To conclude, we perform essentially exact real-time calculation of the spin current through an interacting ESR quantum dot. We benchmark the essentially exact tDMRG result against those from various analytical and approximate methods. From the extracted average spin current, we obtain the Coulomb block shift of the spin current peak, confirmed by the time-dependent Hartree-Fock calculations. We find that the spin current attains its maximum for a spin neutral quantum dot. The spin neutral condition is fulfilled for two gate voltages where V_g matches the magnitude of the rotational magnetic field. The two spin current peaks respond differently to the electronic correlation, the lower filling peak shifts downwards by U while the higher filling peak is nearly unaffected. Comparison to the NEGF approach with an infinite lead shows that the finite-size effect does not affect the qualitative behavior of the quasisteady-state quantities. These results are also compared with those of the TD-HFA approach. It is shown that the TD-HFA gives accurate quasisteady-state dot occupation and spin current. However its prediction on the real-time dynamics is problematic.

ACKNOWLEDGMENTS

The work is supported by NSFC and MOST of China. X.C.X. is supported by U.S. DOE under Grant No. DE-FG02-04ER46124 and the C-SPIN center in Oklahoma. L.W. and H.J. thank P. Zhang for helpful discussions.

¹S. A. Wolf, *Science* **294**, 1488 (2001).

²E. R. Mucciolo, C. Chamon, and C. M. Marcus, *Phys. Rev. Lett.* **89**, 146802 (2002).

³S. K. Watson, R. M. Potok, C. M. Marcus, and V. Umansky, *Phys. Rev. Lett.* **91**, 258301 (2003).

⁴R. M. Potok, J. A. Folk, C. M. Marcus, and V. Umansky, *Phys. Rev. Lett.* **89**, 266602 (2002).

⁵R. Potok, J. A. Folk, C. M. Marcus, V. Umansky, M. Hanson, and A. Gossard, *Phys. Rev. Lett.* **91**, 016802 (2003).

⁶F. H. L. Koppens, C. Buizert, K. J. Tielrooij, I. T. Vink, K. C. Nowack, T. Meunier, L. P. Kouwenhoven, and L. M. K. Vander-sypen, *Nature (London)* **442**, 766 (2006).

⁷G. Vidal, *Phys. Rev. Lett.* **93**, 040502 (2004).

⁸G. Vidal, *Phys. Rev. Lett.* **91**, 147902 (2003).

⁹S. R. White and A. E. Feiguin, *Phys. Rev. Lett.* **93**, 076401 (2004).

¹⁰A. J. Daley, C. Kollath, U. Schollwöck, and G. Vidal, *J. Stat. Mech.: Theory Exp.* **2004**, P04005.

¹¹K. A. Al-Hassanieh, A. E. Feiguin, J. A. Riera, C. A. Büsser, and E. Dagotto, *Phys. Rev. B* **73**, 195304 (2006).

¹²S. Kirino, T. Fujii, J. Zhao, and K. Ueda, *J. Phys. Soc. Jpn.* **77**, 084704 (2008).

¹³F. Heidrich-Meisner, A. E. Feiguin, and E. Dagotto, *Phys. Rev. B* **79**, 235336 (2009).

¹⁴L. G. G. V. Dias da Silva, F. Heidrich-Meisner, A. E. Feiguin, C. Büsser, G. B. Martins, E. V. Anda, and E. Dagotto, *Phys. Rev. B*

- 78**, 195317 (2008).
- ¹⁵C. Guo, A. Weichselbaum, S. Kehrein, T. Xiang, and J. V. Delft, *Phys. Rev. B* **79**, 115137 (2009).
- ¹⁶F. B. Anders and A. Schiller, *Phys. Rev. Lett.* **95**, 196801 (2005).
- ¹⁷C. Karrasch, T. Enss, and V. Meden, *Phys. Rev. B* **73**, 235337 (2006).
- ¹⁸F. Heidrich-Meisner, G. B. Martins, C. Büsler, K. A. Al-Hassanied, A. E. Feiguin, G. Chiappe, E. V. Anda, and E. Dagotto, *Eur. Phys. J. B* **67**, 527 (2009).
- ¹⁹S. Kehrein, *Phys. Rev. Lett.* **95**, 056602 (2005).
- ²⁰D. Lobaskin and S. Kehrein, *Phys. Rev. B* **71**, 193303 (2005).
- ²¹M. Schiró and M. Fabrizio, *Phys. Rev. B* **79**, 153302 (2009).
- ²²T. L. Schmidt, P. Werner, L. Mühlbacher, and A. Komnik, *Phys. Rev. B* **78**, 235110 (2008).
- ²³P. Werner, T. Oka, and A. J. Millis, *Phys. Rev. B* **79**, 035320 (2009).
- ²⁴F. Verstraete, V. Murg, and J. I. Cirac, *Adv. Phys.* **57**, 143 (2008).
- ²⁵P. Zhang, Q.-K. Xue, and X. C. Xie, *Phys. Rev. Lett.* **91**, 196602 (2003).
- ²⁶K. Hattori, *Phys. Rev. B* **75**, 205302 (2007).
- ²⁷K. Hattori, *Phys. Rev. B* **78**, 155321 (2008).
- ²⁸F. Verstraete, J. J. Garcia-Ripoll, and J. I. Cirac, *Phys. Rev. Lett.* **93**, 207204 (2004).
- ²⁹H. Saberi, A. Weichselbaum, and J. V. Delft, *Phys. Rev. B* **78**, 035124 (2008).
- ³⁰P. Myöhänen, A. Stan, G. Stefanucci, and R. van Leeuwen, *EPL* **84**, 67001 (2008).
- ³¹K. Balzer, M. Bonitz, R. van Leeuwen, A. Stan, and N. E. Dahlen, *Phys. Rev. B* **79**, 245306 (2009).
- ³²P. Myöhänen, A. Stan, G. Stefanucci, and R. van Leeuwen, *Phys. Rev. B* **80**, 115107 (2009).